LOAD TRANSFER ALONG THE BONE-DENTAL IMPLANT INTERFACE

Samira Faegh and Sinan Müftü
Northeastern University
Department of Mechanical Engineering
Boston, MA 02115

ABSTRACT

In this paper the variation of normal and shear stresses along a path defined on the bone dental-implant interface is investigated. In particular, the effects of implant diameter, collar length and slope, body-length, and the effects of four different types of external threads on the interfacial stress distribution are studied. The geometry of the bone is digitized from a CT-scan of a mandibular incisor and the surrounding bone. The bone and the implant are assumed to be perfectly bonded. The finite element method with 2D plane strain assumption is used to compute the interfacial stresses. Highest continuous interfacial stresses are encountered in the region where the implant collar engages the cortical region, and near the apex of the implant in the subcortical region. Stress concentrations in the interfacial stresses occur near the geometric discontinuities on the implant contour, and jump in stress values occur where the elastic modulus of the bone transitions between the cortical and trabecular bone. Among the six contour parameters, the slope and the length of the implant collar, and the implant diameter influence the interfacial stress levels the most, and the effects of changing these parameters are only significantly noticed in the cortical bone (alveolar ridge) area. External threads cause significant stress concentrations in interfacial stresses in otherwise smoothly varying regions. This work shows that the presence of external threads could cause significant variations in both normal and shear stresses along the bone-implant interface; but not the reduction in shear stress as previously thought.

INTRODUCTION

A dental implant is a prosthetic device made of alloplastic material, usually commercially pure titanium or Ti-6Al-4V, implanted within the bone to provide retention and support for a fixed or removable prosthesis. The implant treatment protocol involves surgical placement of the implant into an osteotomy site. Osseointegration takes a typical healing period of 3-6 months. A prosthetic tooth is then attached to the implant via an abutment (Bozkaya and Müftü, 2003). Bone healing around a dental implant has three phases, starting with the growth of woven bone around the implant after the implant placement, and lasting for four to six weeks. In the next phase, lamellar bone replaces the woven bone, starting in the second month. Bone remodeling is the third phase, which starts around the third month and continues for the rest of life (Schenk and Buser, 2000).

Different factors influence osseointegration in each one of these phases. Sufficient blood supply, precise, non-traumatized implant receptor site, and initial mechanical stability provided by an implant design that allows no micro-movement between bone and a biocompatible implant material are important factors during the initial healing period. In the third phase, bone

maintenance around the implant is influenced by the load transferred from the implant to the bone, through the remodeling process (Carter and Beaupre, 2001). In this phase, the extent of bone implant contact (BIC) along the bone-implant interface (BII), magnitude and direction of the forces acting on the implant, and the contour shape of the implant are the critical factors (Akpinar et al., 1996).

Osseointegration implies attachment between the bone and the implant along the BII (Brunski, 1983; Skalak, 1988; Rieger et al., 1989). Whether the attachment is enabled through interlocking between the surface asperities and the bone or through chemical or physical bonds is not clear. Numerical analysis of bone implant interaction implies that both shear and normal stresses should be transferable along the interface (Brunski, 1983; Skalak, 1988). Recently, Shim *et al.* (2009) measured the tensile strength of the bone-Ti interface using laser spallation technique as a function of surface roughness and treatment. Indirect estimates of the interfacial shear strength have been made in pull-out and/or torque studies following implantation in animals, where some experiments show failure in the bone, and others along the BII. A strong trend of increasing shear strength of the BII (Ti) with increasing roughness has been reported, with the interfacial shear strength in the 2 – 14 MPa range (Shalabi et al., 2006).

A large number of successful implant designs varying in shape, size, materials and contours have been developed. In particular, implants with external threads find high use as they provide better initial stability. The thread shape plays an important role in load transfer from dental implant to the surrounding bone (Schenk and Buser, 2000). Rounding off the corners of the implant and the threads reduce the stress concentrations (Siegele and Soltesz, 1989; Romanos, 2005). Square threads reduce the bone level stresses (Misch et al., 1998; Chun et al. 2002). Use of different thread configurations for different bone qualities have been suggested (Misch et al., 1998; Romanos 2005). Hansson (1999) showed that the threaded collar implant design transfers lower interfacial shear stresses to the bone. Various systematic studies of the effects of implant contour, on the load transfer from the implant to the cortical and trabecular bone show that most of the external force is transferred to the cortical bone (Holmgren et al. 1998; Rieger et al., 1989; Siegele and Soltesz, 1989; Chun Et al. 2002; del Valle et al. 1997; Bozkaya et al., 2004).

Considerable amount of experimental and numerical studies have been performed on understanding the mechanism of load transfer from the implants to the bone. The initial stability of the implant, the stimulation (mechanotransduction) of the bone cells for healing and maintenance, the long term strength of the BII all depend on the load transfer characteristics along the BII. Despite its significance the exact nature of load transfer along the BII received very little attention, except for Siegele and Soltesz (1989), and Akpinar et al. (1996). Analytical investigations of the interfacial stresses between bonded elastic wedges (Bogy, 1968), and load transfer characteristics from a bar embedded in an elastic half space (Lee and Murata, 1994; Muki and Sternberg, 1970) are limited to simple geometries. Load transfer in the BII is complicated due to the complex morphology of the external and internal bone contours; and, the fact that implant contours deviate considerably from simple cylinders. In this work effects of implant contour on the load transfer along the BII are investigated.

MATERIALS AND METHODS

Two main features defining the shape of a dental implant are its general contour, and its external threads, which are investigated in this work. The implant contour can be partitioned to

four main parts (Figure 1a): the *collar region*, the *body-1 region*, the *body-2 region*, and the *apex region*. The geometry of these regions is defined by six parameters: the length, L_c, and the slope θ_c of the collar region, the length, L_{b1}, and the diameter, D, of the body-1 region, and the length, L_{b2}, and the slope, θ_{b2}, of the body-2 region. The values of these parameters are given in Table 1. The apex of the implant is flat (Figure 1a) in this work. In order to standardize the effect of the abutment, its diameter and protrusion height are kept at 3 mm and 5 mm, respectively, for all implants, and the implant-to-abutment connection is assumed to be monolithic (Figure 1a). The key points (A – J) of the implant geometry, defined with respect to the (x, y) coordinate system are described in Table 2.

Four thread types, shown in Figure 2, are modeled. The geometry of the thread is defined by three parameters: the *thread pitch*, p_t, the *thread depth* h_t, and the *thread slope* θ_t. Dimensions used for these parameters are given in Table 3. The thread depth, h_t, and the thread pitch, p_t, are designated to be 0.32 mm and $L_{b1}/7$, respectively, for all four cases. The thread slope values are defined as shown in Figure 2, as follows: $\theta_1 = \mathrm{atan}(2h_t / p_t)$, $\theta_3 = \mathrm{atan}(p_t / 3h_t)$ and $\theta_2 = \theta_4 = \mathrm{atan}(3h_t / p_t)$.

A bone cross-section of the buccal-lingual (BL) plane was obtained from a CT scan, near a mandibular incisor (Figure 1b) and digitized in MATLAB (Natick, MA, USA). An ANSYS ver. 11 (Canonsburg, PA, USA) macro was written to automatically create the bone and the implants. Close inspection of the buccal side of the alveolar ridge region of the CT scan (Figure 1a) shows loss of buccal cortical plate around the natural tooth. Bone augmentation is a common part of the treatment protocol. Two different amounts of augmentation, one that is 4 mm thick (Figure 1c) and another that is 1.5 mm thick were modeled. All the components and the bone were assumed to be perfectly bonded. A path, s, was defined along the BII staring from point A and ending at point J, (Figure 1a). The stress components, $\{\sigma_x, \sigma_y, \tau_{xy}\}$ with respect to the (x, y) coordinate system, were extracted from the results of the finite element analysis. The stresses components σ_{11} and σ_{12} that are normal and tangential to the interfacial path of the BII, as shown in Figure 1a, were evaluated by using stress transformation relationships (Hibbeler, 2004). The normal $\vec{n}_1$ and tangent $\vec{n}_2$ vectors of the path are oriented as shown in Figure 1a. The orientation θ of the path with respect to the x-axis is computed from the contour geometry. The positive direction of the interfacial stress components σ_{11} and σ_{12} for a given θ is also depicted in Figure 1a.

The PLANE 42, solid element of ANSYS was used with plane strain assumption. When this assumption is used the geometry is assumed to be very long compared to the planar dimensions and the external forces are uniformly distributed in the length direction. This assumption was necessary as the number of elements, that were required to obtain a very detailed resolution of the abrupt stress changes, were very large. The element size adjacent to the BII was 0.0125 mm. Other regions were meshed according to their distance to the BII, with 0.05 and 0.4 mm elements (Figure 2). The analyses involved approximately 206,000 elements for the cases that involved threads, and approximately 180,000 elements for the non-threaded implants. Bone was restricted in all degrees of freedom along the inferior periphery (Figure 1c). The biting force on the prosthesis was modeled by applying 18.8 N/mm distributed force at the center of abutment, oriented 11 degrees with respect to the main axis. Considering an occlusal width of 6 mm, this load amounts to 113 N normal force acting on the abutment (Bozkaya et al., 2004). In

addition, a bending moment of the amount 90 N.mm was applied, similarly, on the abutment in order to transfer the load from the occlusal load center to the abutment as shown in Figure 1c. The implant, and the cortical and trabecular bone regions were assumed to behave elastically, with moduli 113, 13 and 1 GPa, respectively, and Poisson's ratio 0.3 (Lemons and Dietsh-Misch, 1999). A comparison of the results for the full 3D and the 2D plane strain case was carried out (Faegh, 2009). This showed that the stress magnitudes predicted by using a 2D plane strain analysis are on the same order of magnitude in the BL-plane.

RESULTS

First, the load transfer characteristics between an implant without external threads and the bone are presented. The dimensions of this implant are θ_c = -10 degrees, L_c = 1 mm, L_{b1} = 5 mm, L_{b2} = 3 mm, θ_{b2} = 5 degrees, D = 3.3 mm. Unless otherwise noted these dimensions form the base values in the paper. Figure 3 shows the von Mises (vM) stress distribution in the bone as well as the interfacial normal σ_{11} and shear σ_{12} stresses along the BII. Note that the implant is placed in the cortical bone slightly more lingual than the original position of the root, following common implant dentistry practice to have better stability of the implant, and avoid fenestration of the labial cortical bone. High vM-stresses develop on the buccal side of the cortical bone, and a stress concentration region develops near implant apex, points G and F. Trabecular bone bears relatively low levels of stress. Nevertheless, close to the BII the vM-stress is higher than the inferior section of the trabecular region. Stress drops to zero near the inferior aspect of the mandible, but this is influenced by the fixed boundary conditions (Faegh, 2009).

Figure 3b shows that interfacial normal stress σ_{11} is primarily compressive on the buccal side of the collar region, but it becomes tensile on the lingual side. A small jump in the normal stress is observed at point B, where the contour slope changes between the collar and body regions. A stress concentration occurs at point C, at s = 4 mm, where the bone transitions from compact to trabecular. Similar stress concentrations are observed at the apical corners of the implant, particularly on the lingual side. Figure 3c shows that the direction of the shear stress σ_{12} is primarily the same in all regions of the BII, but directional changes occur, near the implant's apex due to implant geometry change, and bone transition at points F and G. On the buccal side of the collar region, the shear stress increases gradually. A jump occurs at point B, s~1 mm due to geometry, and at point C, s~4 mm, due to bone transition. Similar observations are made for the collar region on the lingual side of the interface. Body-1 and body-2 regions of the implant bear relatively small levels of shear stress. The variation of the normal and shear stresses in the BII are plotted schematically on the insets in Figure 3, and provide a visual interpretation of the orientation and magnitudes of the interfacial loading conditions.

The implant contour is defined by six geometric parameters (L_c, θ_c, L_{b1}, D, L_{b2}, θ_{b2}). Analysis, carried for the parameters given in Table 1, showed that significant changes in interfacial stresses occur only with the implant diameter (D), and the collar parameters θ_c and L_c, which are presented next.

The effects of collar slope are presented for θ_c=-10,0 and 10 degrees, for D = 3.3,3.5,4 mm, and for bone graft amounts of 4 and 1.5 mm, in Figures 4 and 5, respectively. The interfacial stresses σ_{11} and σ_{12} along the BII are presented, in the range $0 \leq s \leq 5$ mm, corresponding to superior, buccal region of the interface. In both cases, the length of the implant collar L_c is 1 mm, and it is entirely surrounded by cortical bone. Comparison of Figures 4a/5a and 4c/5c shows that, in the collar region, $0 \leq s \leq 1$ mm, both of the interfacial normal and shear

stresses are generally lower for the implants with positive collar slope (θ_c=10 deg). These figures also show a jump in both σ_{11} and σ_{12} at s =1 mm, where the collar slope changes (point-B). In the case of interfacial normal stress σ_{11} the implants with the negative collar slope (θ_c=-10 deg., in Figures 4a and 5a) experience a reduction at this slope transition point, whereas the implants with positive collar slope (θ_c=10 deg., in Figures 4c and 5c) experience an increase. The end point (B) of the collar region causes a discontinuity and a concentrated stress in the variation of the shear stress as well.

In Figure 4, the body-1 region of the implant is engaged with cortical bone in the range $1 \leq s \leq 4$ mm, and in Figure 5 the extent of this interface is in the range $1 \leq s \leq 1.5$ mm. In the case of the 4 mm long cortical region (Figure 4) both of the interfacial stress components are able to establish relatively wide regions of smoothly varying stress distributions, whereas in the case of the 1.5 mm long cortical region (Figure 5) the stress distribution is greatly affected by the transition boundaries at points B and C. The jump in the interfacial stress magnitudes occur at point C (s=4 and 1.5 mm, in Figures 4 and 5, respectively) due to the change in elastic modulus of the bone from 13 GPa to 1 GPa.

The effect of collar length is investigated for L_c=1, 2 and 3 mm, for the case of θ_c=-10 degrees and for the three different implant diameters. The normal and shear stress components along the BII are presented for 1.5 mm thick cortical bone in Figure 6. Investigating Figures 5a and 6 shows that, using a collar length that is longer than the length of the cortical bone region results in overall reduction of the interfacial normal stress σ_{11} in the cortical bone region, $0 \leq s \leq 1.5$ mm. However, the shear stress in the collar region does not change noticeably with increasing collar length, L_c.

In this study, implant diameters of 3.3, 3.5, and 4 mm were considered. In all the cases, it is observed that increasing implant's diameter results in decreasing the normal and shear stresses along the BII.

In Figure 7, the effects of using the four different external thread types are evaluated, along with a non-threaded implant by plotting the vM-stress distributions. It is seen that the external threads cause some reduction in the vM-stress in the cortical bone, on both (buccal and lingual) sides, and in regions away from the BII. Details of this reduction are plotted in Figure 7a along a path r, which starts on the implant surface and moves radially into the cortical bone. At the same time the relatively uniform vM-stress distribution in the cortical bone is disrupted with frequent variations in the stress magnitude. It appears that all four types of screw threads have a positive effect on reducing the vM-stresses in the cortical bone-region. Note that this behavior is accompanied with a slight increase in implant stress levels.

The interfacial normal σ_{11} and shear σ_{12} stress components are plotted in Figure 8, in the collar region on the buccal side. It is observed the threaded implants cause significant rapid variations in the interfacial stress levels, while preserving some of the loading characteristics of the non-threaded implants, such as the general level of high loads in the superior and apical regions. The interfacial normal and shear stress variations, over the threads located in the trabecular bone regions, are depicted schematically on the insets of Figure 8, and point out that, on the threads, the interfacial shear stress is coupled to the interfacial normal stress and non-zero.

SUMMARY, DISCUSSION AND CONCLUSIONS

In this work, the effects of external contour of a dental implant on the load transfer characteristics along the BII are evaluated. Highest continuous interfacial stresses are encountered in the region where the implant collar engages the cortical bone, and near the apex of the implant in the trabecular bone. Stress concentrations and discontinuities occur near the geometric discontinuities of the implant contour, and the cortical-to-trabecular bone boundary. The interfacial normal stress is generally compressive along the interface. The interfacial shear stress (σ_{12}) has magnitude comparable to the normal stress in the collar regions, and is generally high in the buccal side of the body-regions. Among the six contour parameters, the slope (θ_c) and length (L_c) of the implant collar, and the implant diameter (D) influence the interfacial stress levels the most, and the effects of changing these parameters are only significant in the alveolar ridge region. Positive collar slope, larger implant diameter D, and longer implant collar reduce the magnitudes of the interfacial stresses. The external threads cause significant changes in the interfacial stress magnitudes, but the underlying load carrying characteristics of the interface remain intact. In general, a slight reduction in the interfacial stress values in the cortical bone region can be observed, but the increase due to stress concentrations near the thread corners outweighs this effect.

Externally threaded implants improve primary implant stability during implant insertion (Lemons and Dietsh-Misch, 1999), and reduce micromotion during post insertion healing period. It has been suggested that use of external threads changes the main load carrying mechanism of the BII from one that relies primarily on the shear stresses along the body of the implant, to one that relies primarily on the normal stresses acting on the faces of the threads (Misch et al., 1998; Skalak, 1988; Hansson, 1999). The present work indicates that the situation is more complicated. Both normal and shear stresses along the BII are significantly and equally influenced by the use of the external threads, as they are interdependent. While this work involves several assumptions: a) linear-elastic, plane-strain material behavior; b) the boundary fixation along the inferior bone contour; c) threads with sharp corners; and, d) abrupt transition of material properties at the cortical-to-trabecular bone boundary; nevertheless, the increase of both normal and shear stresses that are transferred along the BII should be considered as a strong possibility, based on the results presented in this work.

The strength of the bone-implant interface is difficult to measure. Analysis presented in this work sheds light into the complex nature of the loading conditions along this interface. In several finite element studies the BII was modeled as a contact interface with the shear strength lumped into a friction coefficient, and in others cohesive elements with finite tensile strength have been used (Wakayabashi et al., 2008; Lin et al., 2009). In this first systematic study of the exact stress distribution along the BII, we assumed a perfect osseointegration. The effects of finite cohesive properties of the interface can be carried out in the future.

Histomorphometric studies of dental implant systems show less than 100% BIC in subperiosteal areas, and low levels of bone formation between the threads (e.g., Romanos, 2005; Schenk and Buser, 2000). The results of this work can also be used to shed light onto this less than perfect BIC. This work showed that for the threadless-implants, or for the non-threaded segments of the threded-implants, the interfacial load levels in trabecular bone, along the body-1 and body-2 regions (Figures 3b,c and 8a), could be too low for adequate bone stimulation (Frost, 1987). Evidence of insufficient bone stimulation for long term bone maintenance in implants without external threads was demonstrated in a recent bone remodeling study (Chou et al., 2008),

and it has also been shown in histomorphology studies (Schenk and Buser, 2000; Albrektsson et al., 1986). On the other hand, the increased interfacial loading of the bone due to the external threads can be indicative of increased remodeling activity.

ACKNOWLEDGEMENT

The authors would like to thank Dr. Ali Müftü from Tufts University for helpful discussions related to this work.

REFERENCES

1. Akpinar, I., Demirel, F., Parnas, L., P., Sahin, S., 1996. A comparison of stress and strain distribution characteristics of two different rigid implant designs for distal-extension fixed prostheses. Quintessence International 27, 11-17.
2. Albrektsson, T. Zarb, G. Worthington, P. Eriksson, AR., 1986. The long term efficacy of currently used dental implants. A review and proposed criteria for success. The International Journal of Oral & Maxillofacial Implants 1, 11-25.
3. Bogy, D.B., 1968. Edge bonded dissimilar orthogonal elastic wedges under normal and shear loading. Journal Applied Mechanics 35, 460-466.
4. Bozkaya, D., Müftü, S., Müftü, A., 2004. Evaluation of load transfer characteristics of five different implants in compact bone at different load levels by finite element analysis. The Journal of Prosthetic Dentistry 92, 523-530.
5. Bozkaya, D. Müftü, S., 2003. Mechanics of the tapered interference fit in dental implants. Journal of Biomechanics 36, 1649-58.
6. Brunski, JB., 1999. In vivo bone response to biomechanical loading at the bone/dental-implant interface. Advances in Dental Research 13, 99-119.
7. Brunski, J.B. Hipp, J.A., Shepard, M.S., Cochran, G.V.B., 1983. Modeling the bone-implant interface in a study of interfacial bone adaptation/damage. In Advances in Bioengineering, ASME, N.Y., 43-44.
8. Carter, D.R. Beaupre, G.S., 2001. Skeletal Function and Form: Mechanobiology of Skeletal Development, Aging, and Regeneration, Cambridge University Press, Cambridge.
9. Chou, H.-Y., Jagodnik, J.J. Müftü, S., 2008. Predictions of bone remodeling around dental implant systems. Journal of Biomechanics 41, 1365-1373.
10. Chun, H.J., Cheong, S.Y., Han, J.H., Heo, S.J., Chung, J.P., Rhyu, I.C., Choi, Y.C., Baik, H.K., Ku, Y., Kim, M.H., 2002. Evaluation of design parameters of osseointegrated dental implants using finite element analysis. Journal of Oral Rehabilitation 29, 565-574.
11. Del Valle., V., Faulkner, G., Wolfaardt, J., Dent, M., 1997. Craniofacial osseointegrated implant-induced strain distribution: A numerical study. The International Journal of Oral and Maxillofacial Implants 12, 200-210.
12. Faegh, S., 2009. Mechanism of Load Transfer along the Bone Dental-Implant Interface. M.S. Thesis, Northeastern University, Boston, MA.
13. Frost, H.M., 1987. Bone "mass" and the "mechanostat": a proposal. The Anatomical Record 219, 1-9.
14. Hansson, S., 1999. The implant neck: smooth or provided with retention elements: A clinical study. Oral Implants Research 10, 394-405.
15. Hibbeler, R.C., 2004. Mechanics of Materials, Pearson, Prentice-Hall, Upper Saddle River, N.J., p. 458.

16. Holmgren, E.P., Seckinger, R.J., Kilgren, L.M., Mante, F., 1998. Evaluating parameters of osseointegrated dental implants using finite element analysis- a two-dimensional comparative study examining the effects of implant diameter, implant shape, and location. Journal of Oral Implantology 14, 80-88.

17. Lee, V.G., Mura, T., 1994. Load transfer from a finite cylindrical fiber into an elastic half-space. Journal of Applied Mechanics 61, 971-975.

18. Lemons, J.E., Dietsh-Misch, F., 1999. Biomaterials for dental implants. In: Misch, C.E. (Ed.), Contemporary Implant Dentistry. Mosby, St. Louis, pp. 271-302.

19. Li, J., Li, H., Shi, L., Fok, A.S., Ucer, C., Devlin, H., Horner, K., Silikas, N., 2007. A mathematical model for simulating the bone remodeling process under mechanical stimulus. Dental Materials 23, 1073-1078.

20. Lin, D., Li, Q., Li, W., Swain, M., 2009. Dental implant induced bone remodeling and associated algorithms. Journal of Mechanical Behavior of Biomedical Materials 2, 410-432.

21. Misch, C.E., 1999. Implant design considerations for the posterior regions of the mouth. Implant Dentistry 8, 376-86.

22. Misch, C.E., Hoar, J., Beck, G., Hazen, R., Misch, C.M., 1998. A bone quality based implant system: a preliminary report of stage I & stage II. Implant Dentistry 7, 35-42.

23. Moser, W., Nentwig, G.H., 1989. Finite element studien zur optimierung von implantat-gewindeformen. Z Zhanarztl Implantol 5, 29-32.

24. Muki, R., Sternberg, E., 1970. Elastostatic load-transfer to a half-space from a partially embedded axially loaded rod. International Journal of Solids Structures 6, 69-90

25. Rieger, M.R., Fareed, K., Adams, W.K., Tanquist, R.A., 1989. Bone stress distribution for three endosseous implants. The Journal of Prosthetic Dentistry 61, 223-8

26. Romanos, G., 2005. Immediate Loading of Endosseous Implants in the Posterior Area of the Mandible. Quintessence Books, Berlin.

27. Sato, Y., Shindoi, N., Hosokawa, R., Tsuga, K., Akagawa, Y., 2000. Biomechanical effects of double or wide implants for single molar replacement in the posterior mandibular region. Journal of Oral Rehabilitation 27, 842-5.

28. Schenk, R.K., Buser, D., 2000. Osseointegration: a reality. Periodontology 17, 22-35.

29. Shalabi, M.M., Gortemaker, A., Van't Hof, M.A., Jansen, J.A., Creugers, N.H.J., 2006. Implant surface roughness and bone healing: a systematic review. Critical Reviews in Oral Biology and Medicine 85, 496-500.

30. Shim, J., Nakamura, H., Ogawa, T., Gupta, V., 2009. An understanding of the mechanism that promotes adhesion between roughened titanium implants and mineralized tissue. Journal of Biomechanical Engineering 131, 1-9.

31. Siegele, D., Soltesz, U., 1989. Numerical investigations of the influence of implant shape on stress distribution in the jaw bone. International Journal of Oral Maxillofacial Implants 4, 333-340.

32. Skalak, R., 1988. Stress transfer at the implant interface. Journal of Oral Implantology 13, 531-593.

33. Wakayabashi, N., Ona, M., Suzuki, T., Igarashi, Y., 2008. Nonlinear finite element analysis: Advances and challenges in dental applications. Journal of Dentistry 36, 463-471.

Length of Collar, L_c (mm)	1, 2, 3
Angle of Collar, θ_c (degree)	-10, 0, 10
Length of body-1, L_{b1} (mm)	4, 5, 6
Diameter of body-1, D	3.3, 3.5, 4
Length of body-2, L_{b2} (mm)	3, 4
Angle of body-2, θ_{b2} (degree)	0, 5, 10

Table 1 Implant dimensions that were varied in this work. See Figure 1a for the definitions of these variables. Note that θ_c as drawn in this figure is defined to be a negative angle, whereas θ_{b2} is defined to be positive.

	x	y
A	$D/2 - L_c \tan\theta_c$	0
B	$D/2$	$-L_c$
D	$D/2$	$-(L_c + L_{b1})$
E	$D/2 - L_{b2} \tan\theta_{b2}$	$-(L_c + L_{b1} + L_{b2})$
G	$-D/2 + L_{b2} \tan\theta_{b2}$	$-(L_c + L_{b1} + L_{b2})$
H	$-D/2$	$-(L_c + L_{b1})$
I	$-D/2$	$-L_c$
J	$-D/2 + L_c \tan\theta_c$	0

Table 2 Coordinates of the key points of the implant geometry described in Figure 1a.

Length of body-1 L_{b1} (mm)	Thread depth, h_t (mm)	Thread pitch, p_t (mm)
4	0.32	0.57
5	0.32	0.70
6	0.32	0.85

Table 3 Dimensions of screw threads used in this study
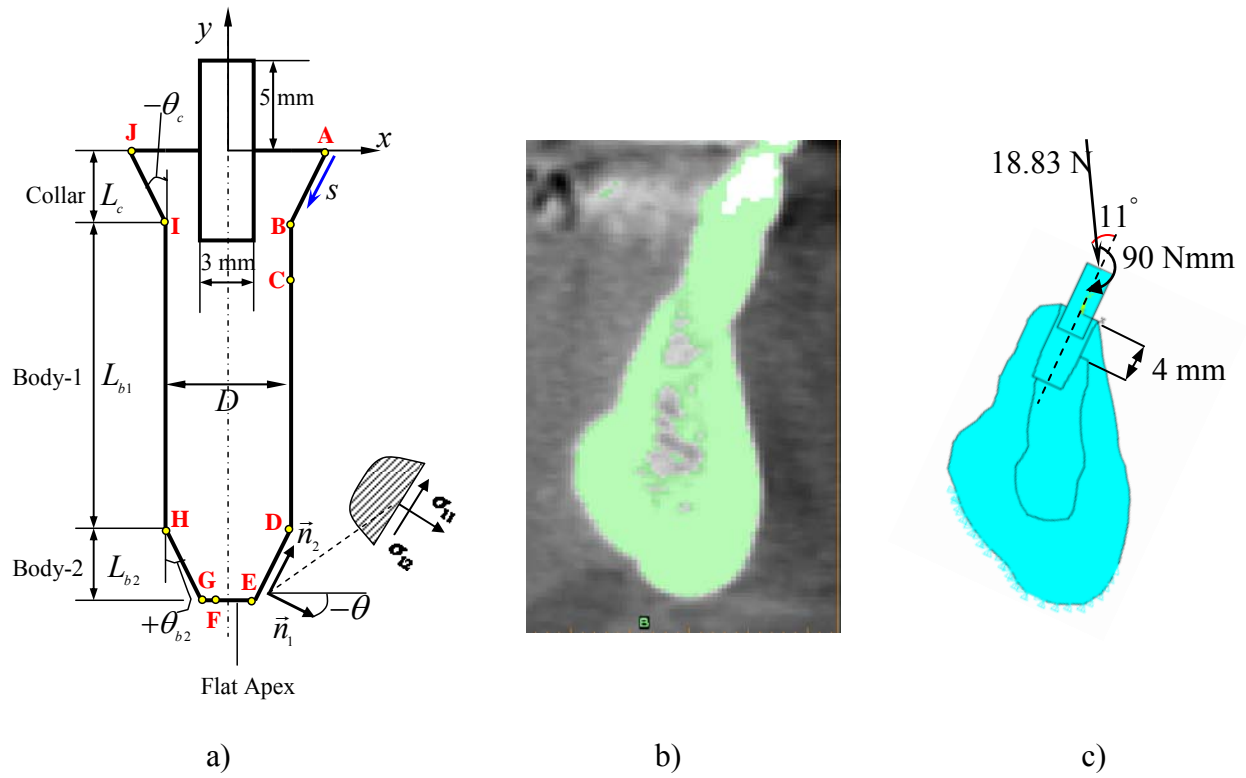
Figure 1 (a) implant dimensions, (b) CT scan of incisor, (c) model created in ANSYS.
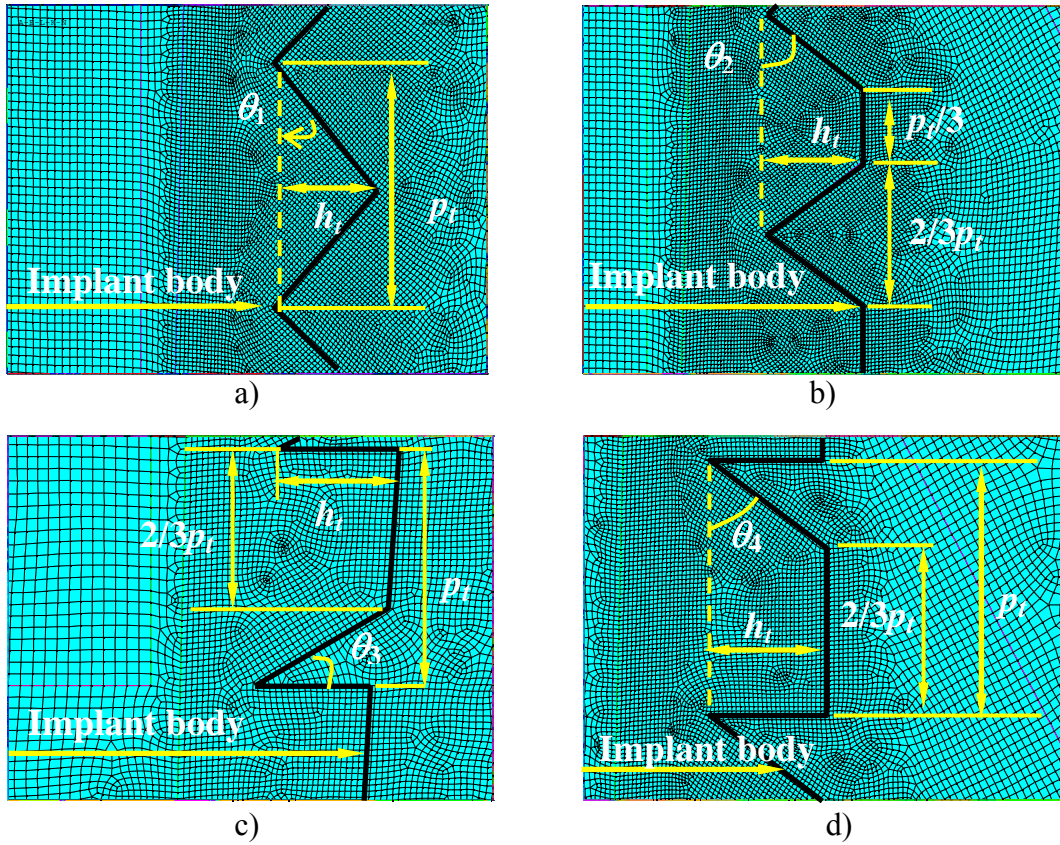
Figure 2 The description of the thread shapes (a) type-1, (b) type-2, (c) type-3 and (d) type-4 and the definitions of thread pitch p_t, and depth h_t. The finite element mesh for each thread is also shown.
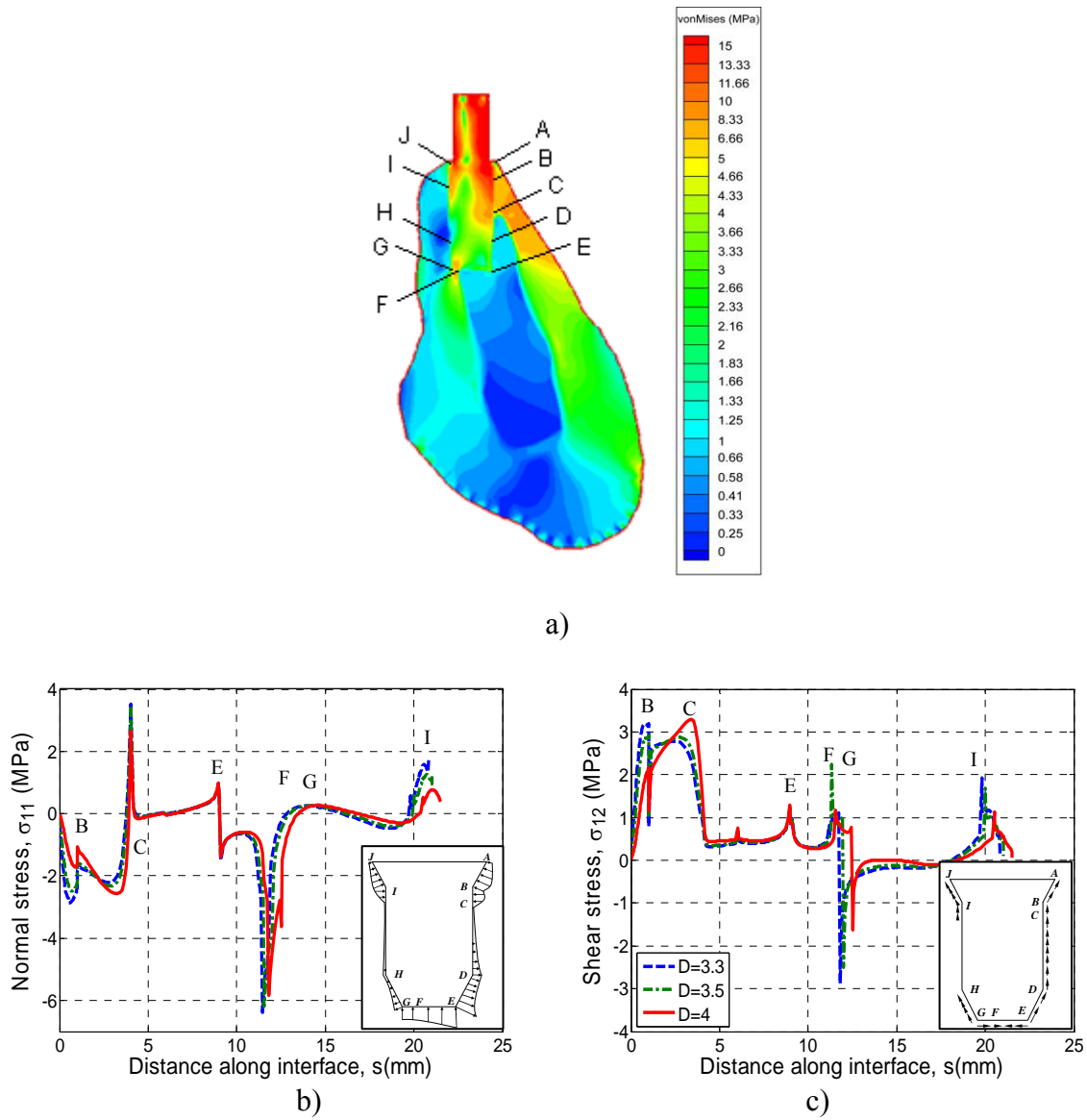
Figure 3 a) von Mises stress distribution, b) normal (σ_{11}) and c) shear stress (σ_{12}) variations along the implant-bone interface (s) for an implant with dimensions $L_{b1} = 5$ mm, $L_c = 1$ mm, $\theta_c = -10$ degree, $L_{b2} = 3$ mm, $\theta_{b2} = 5$ degree.
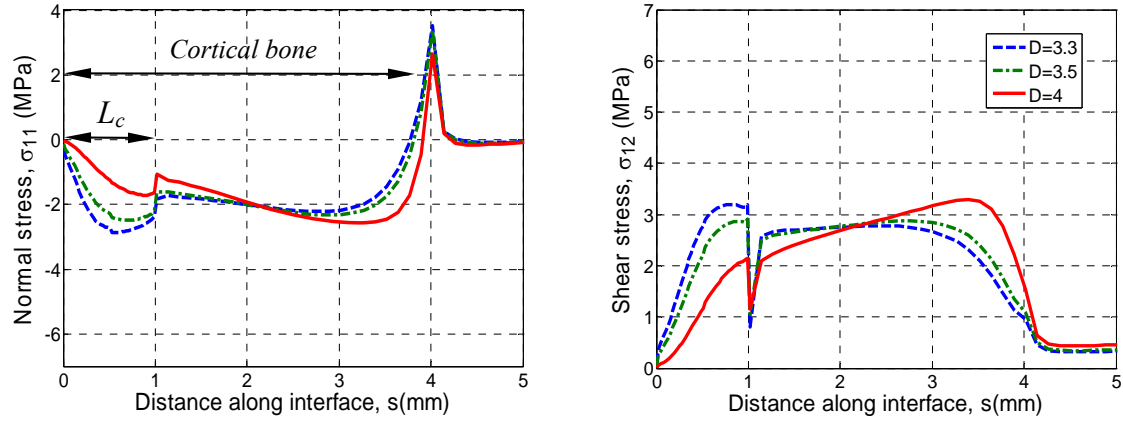
a) $\theta_c = -10\,\mathrm{deg}.$
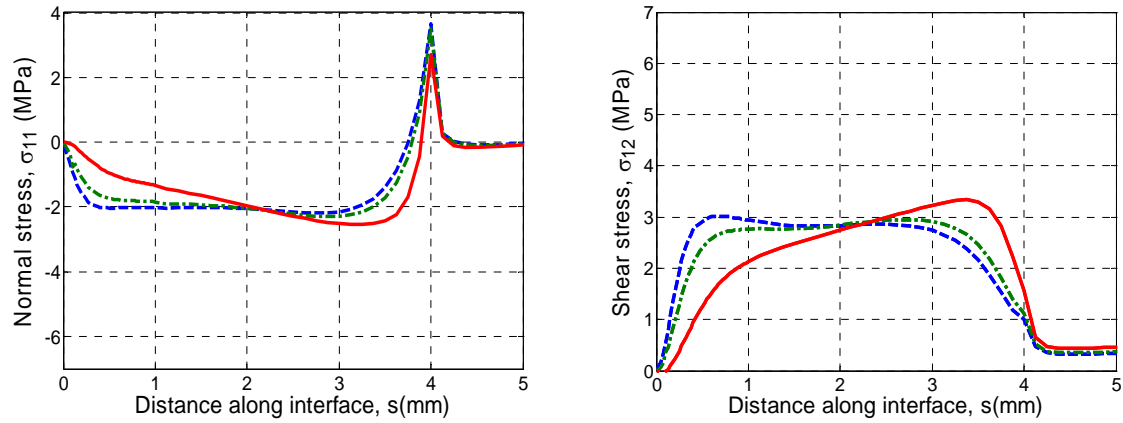
b) $\theta_c = 0\,\mathrm{deg}.$
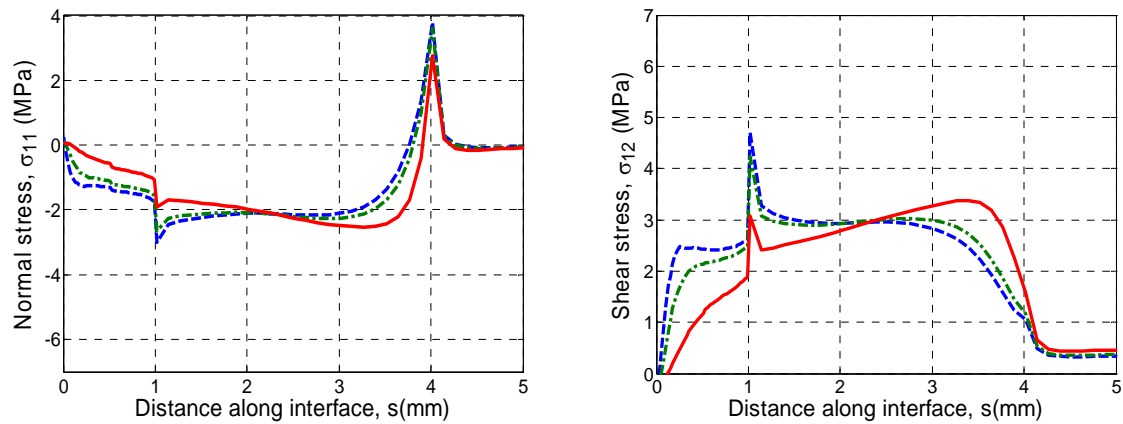
c) $\theta_c = 10\,\mathrm{deg}.$

Figure 4 Effect of the collar slope θ_c on the normal and shear stresses along the bone-implant interface (on the buccal side) for the 4 mm thick cortical bone case, where a) $\theta_c = $ -10 degrees, b) $\theta_c = 0$, c) $\theta_c = 10$ degrees, $L_c = 1$ mm and $D = 3.3.\ 3.5,\ 4$ mm. Other parameters of the implant are as follows: $L_{b1} = 5$ mm, $L_{b2} = 3$ mm, $\theta_{b2} = 5$ degrees.

a) $\theta_c = -10 \deg$.

b) $\theta_c = 0 \deg$.
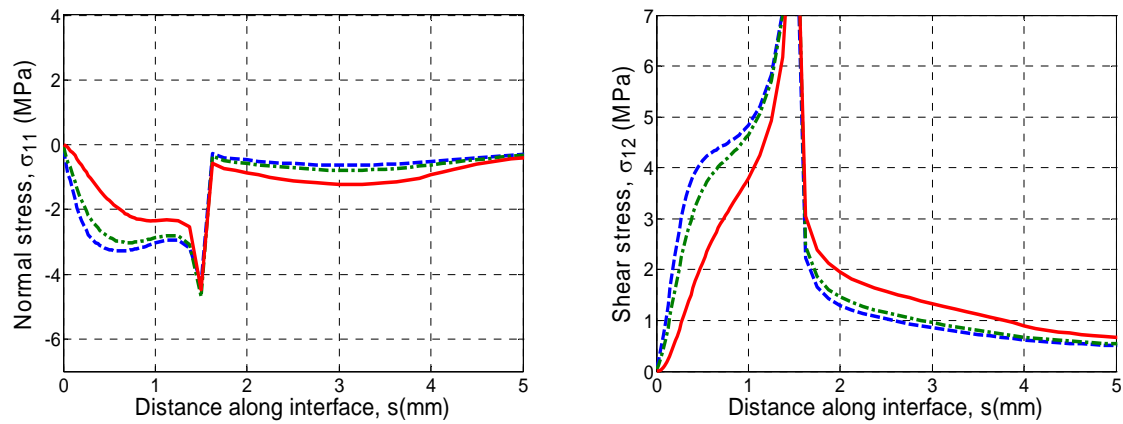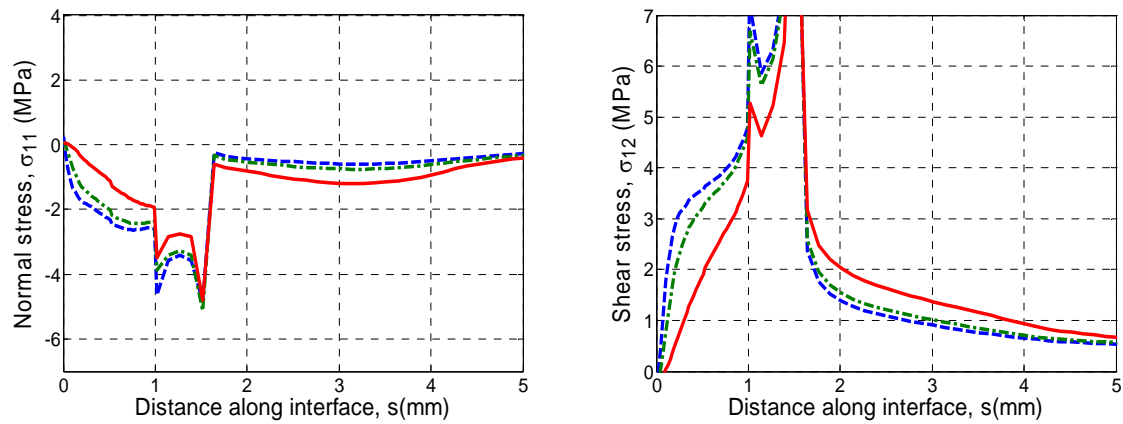
c) $\theta_c = 10 \deg$.

Figure 5 Effect of the collar slope θ_c on the normal and shear stresses along the bone-implant interface (on the buccal side) for the 1.5 mm thick cortical bone case, where a) $\theta_c = $ -10 degrees, b) $\theta_c = 0$, c) $\theta_c = 10$ degrees, $L_c = 1$ mm and $D = 3.3$. 3.5, 4 mm. Other parameters of the implant are as follows: $L_{b1} = 5$ mm, $L_{b2} = 3$ mm, $\theta_{b2} = 5$ degrees.

a) $L_c = 1$ mm
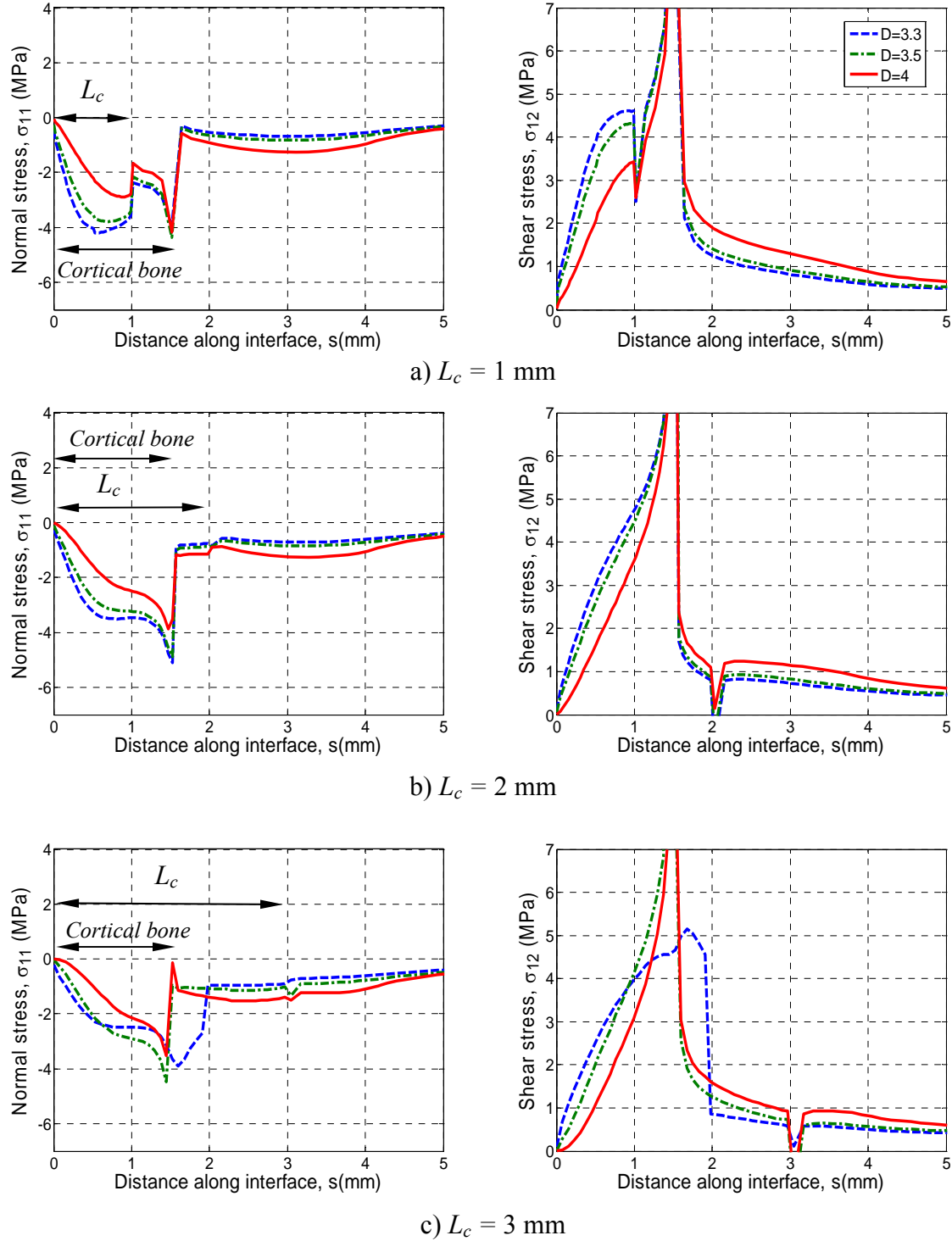
b) $L_c = 2$ mm

c) $L_c = 3$ mm

Figure 6 Effect of the collar length L_c on the normal and shear stresses along the bone-implant interface (on the buccal side) for the 1.5 mm thick cortical bone case, where a) $L_c = 1$ mm, b) $L_c = 2$ mm c) $L_c = 3$ mm, $\theta_c = -10$ deg. and $D = 3.3$. 3.5, 4 mm. Other parameters of the implant are as follows: $L_{b1} = 5$ mm, $L_{b2} = 3$ mm, $\theta_{b2} = 5$ degrees.
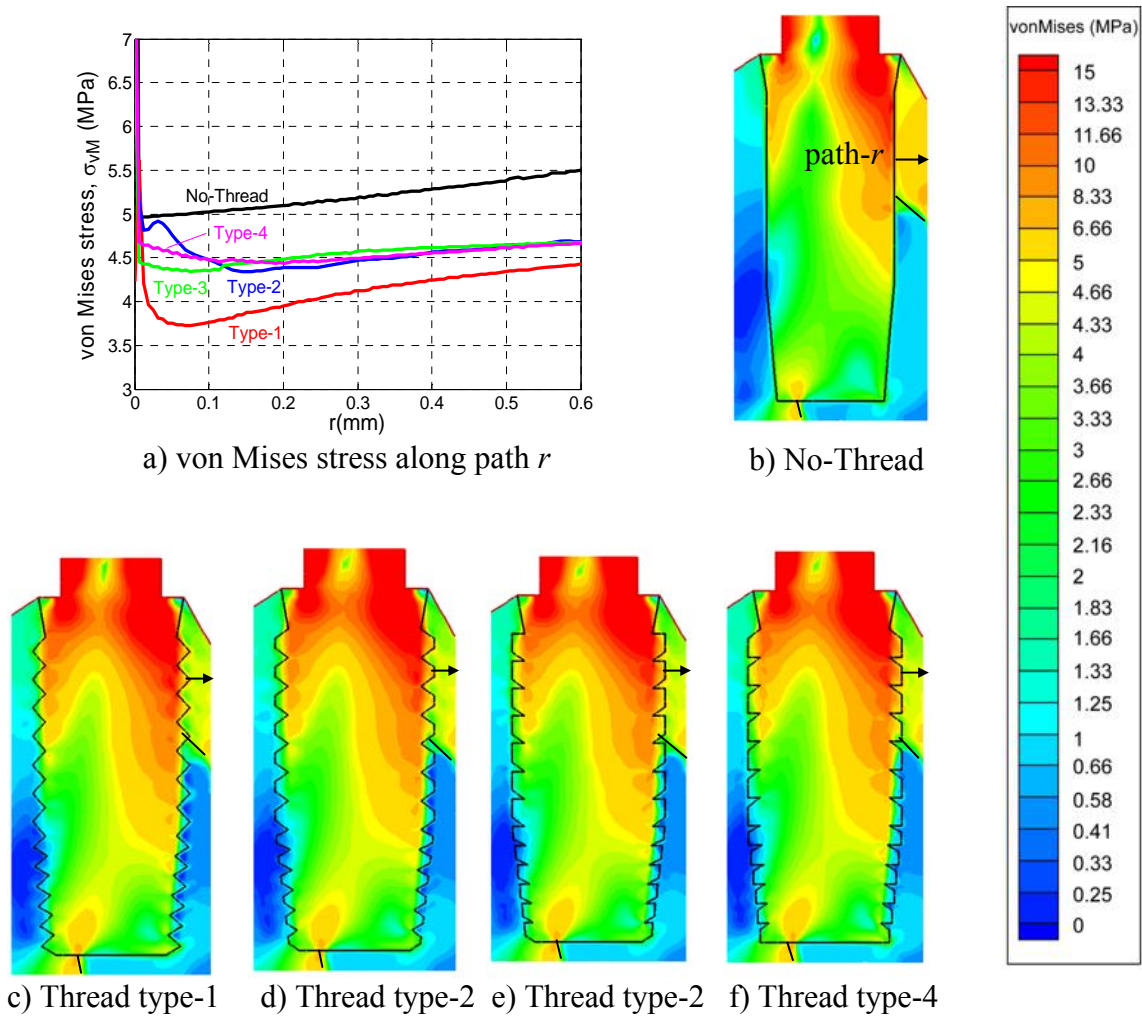
Figure 7 von Mises stress distribution σ_{vM}, around implant for implants with b) no threads, and those with c) Type-1, d) Type-2, e) Type-3, and f) Type-4 threads. a) Shows the change of vM stress along the path-r in the cortical bone, and demonstrates the stress reduction when threaded implants are used along this path.
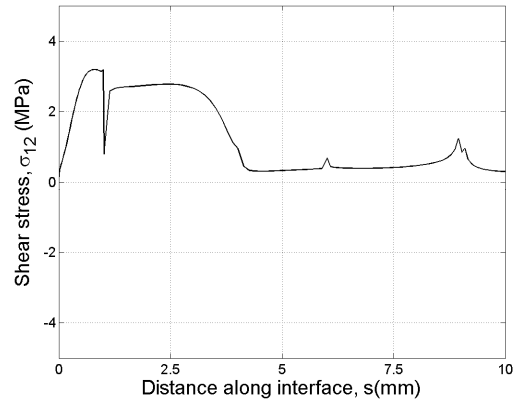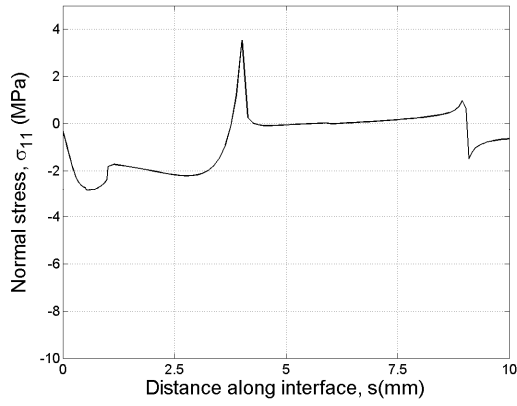
a) No screw
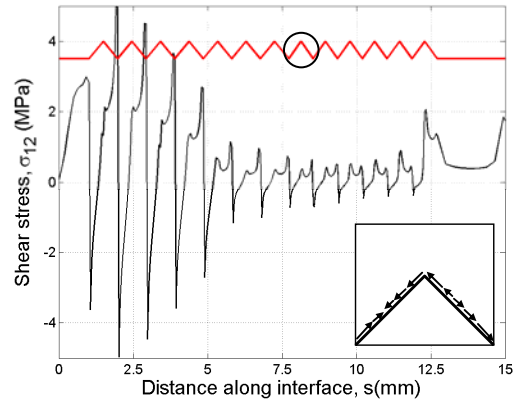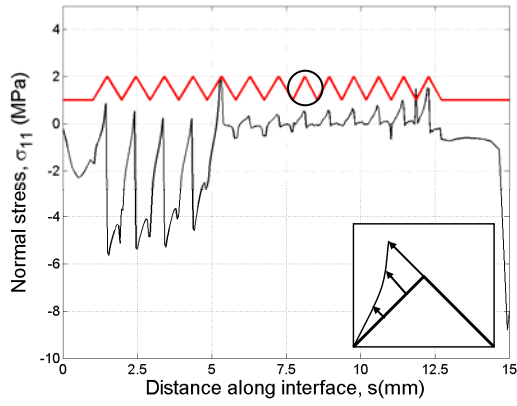
b) Type-1
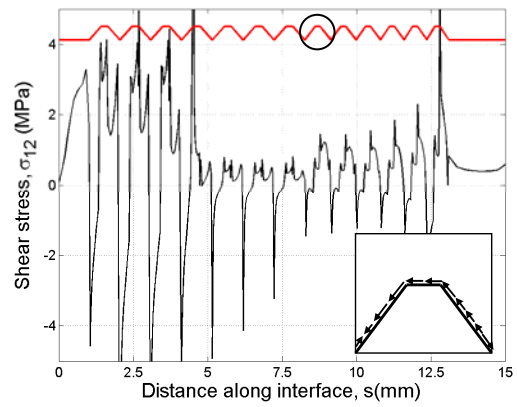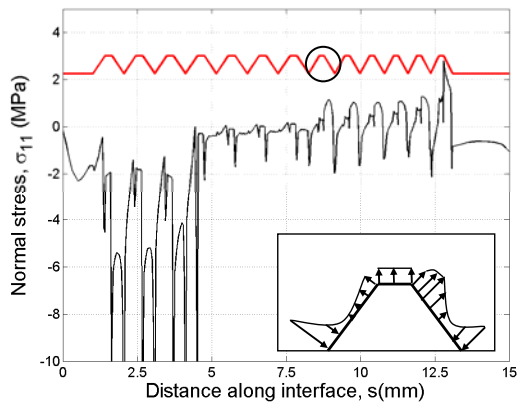
c) Type-2
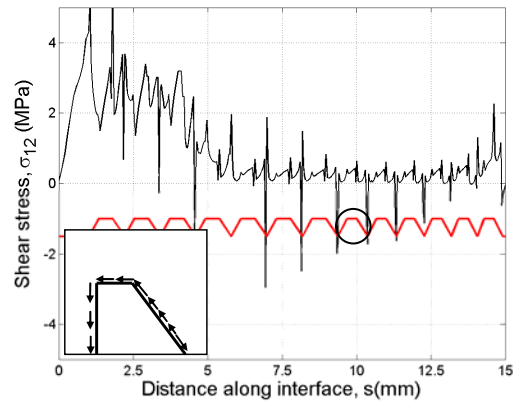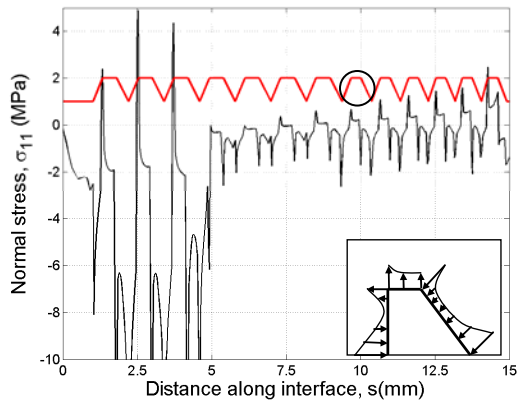
d) Type-3
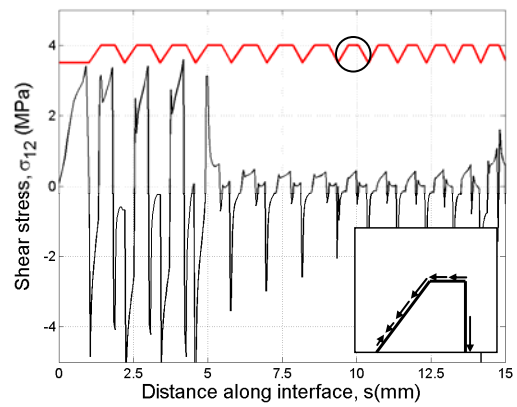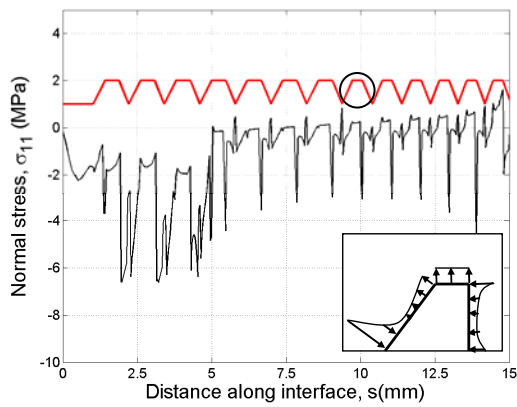
e) Type-4

Figure 8 Normal and shear stress components σ_{11}, σ_{12} along the bone-implant interface (on the buccal side) for implants with a) no-thread, b) Type-1, c) Type-2, d) Type-3, e) Type-4 thread. The other parameters of the implants are as follows: θ_c = -10 degrees, L_c = 1 mm and L_{b1} = 5 mm, L_{b2} = 3 mm, θ_{b2} = 5 degrees, D = 3.3 mm.